Open Journal of Applied Sciences, 2025, 15(1), 53-69
https://www.scirp.org/journal/ojapps
ISSN Online: 2165-3925
ISSN Print: 2165-3917

Modeling of a Parabolic Cylindrical Solar Concentrator

Bati Ernest Boya Bi*, Kpeusseu Angeline Kouambla Epse Yeo, Ekoun Paul Magloire Koffi, Prosper Gbaha

Laboratoire de Mécanique et Sciences des Matériaux, Groupe Energies Renouvelables, Institut National Polytechnique Houphouët Boigny, Yamoussoukro, Côte d'Ivoire
Email: *bati.boyabi@inphb.ci

How to cite this paper: Boya Bi, B.E., Kouambla Epse Yeo, K.A., Koffi, E.P.M. and Gbaha, P. (2025) Modeling of a Parabolic Cylindrical Solar Concentrator. *Open Journal of Applied Sciences*, **15**, 53-69.
https://doi.org/10.4236/ojapps.2025.151005

Received: November 18, 2024
Accepted: January 13, 2025
Published: January 16, 2025

Abstract

This work aims at the mathematical modeling of a parabolic trough concentrator, the numerical resolution of the resulting equation, as well as the simulation of the heat transfer fluid heating process. To do this, a thermal balance was established for the heat transfer fluid, the absorber and the glass. This allowed us to establish an equation system whose resolution was done by the finite difference method. Then, a computer program was developed to simulate the temperatures of the heat transfer fluid, the absorber tube and the glass as a function of time and space. The numerical resolution made it possible to obtain the temperatures of the heat transfer fluid, the absorber and the glass. The simulation of the fluid heating process was done in one-hour time steps, from six in the morning to six in the afternoon. The results obtained show that the temperature difference between the inlet and the outlet of the sensor is very significant. These results obtained, regarding the variation of the temperatures of the heat transfer fluid, the absorber and the glass, as well as the powers and efficiency of the parabolic trough concentrator and various factors, allow for the improvement of the performances of our prototype.

Keywords

Modeling, Simulation, Parabolic Trough Concentrator, Heat Transfer Fluid, Temperature

1. Introduction

The parabolic trough is one of the main technologies currently used in solar thermal power plants for electricity production (operating temperature between 300˚C and 400˚C) and also for heat production for industry (operating temperature between 100˚C and 250˚C) [1].

A lot of research has been done in recent years on the types of solar collectors. While some studies aimed at cost reduction and performance improvement, others focused on improving the reliability of the receiver tube (absorber), the performance of the selective coating and new measurement methods to test the parabolic trough system [2]-[12]. The majority of models are focused on simulation studies. The solar flux and flow rate are generally assumed to be uniform, and many correlations used in the models are also based on a constant temperature. However, due to the non-uniform solar flux on the outer surface of the inner absorber tube, the flow is heated asymmetrically and thus non-uniformly [13] [14]. Balbir *et al.* [2] conducted a sizing study of a parabolic trough concentrator. The study aimed to improve the efficiency and reduce the cost of the solar collector operating with synthetic oil and water. Campo [15] developed a simple algebraic method to improve the heat transfer in turbulent regime in a cylindrical tube for different gases. Grald [16] conducted a parametric study to determine the influence of thermo-physical properties and the performance of the parabolic trough solar collector. Thus, this study aims to model the heat transfer phenomenon in the different compartments of the parabolic trough concentrator. Here, we determine the evolution of the temperature as a function of time by establishing a thermal balance that takes into account the different thermal exchanges, followed by a numerical model based on the following steps [17]:

- The solar energy reflected by the concentrator falls on the absorber;
- The heat is recovered thanks to the heat transfer fluid and it heats up by circulating in the absorber placed under glazing that lets the radiation penetrate and minimizes losses by infrared radiation by using the greenhouse effect. This glazing also makes it possible to limit heat exchanges with the environment.

2. Description

It is presented as a module having a reflector of parabolic shape arranged cylindrically according to **Figure 1**.

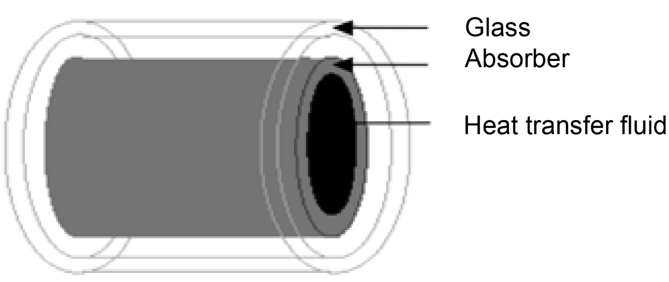

Figure 1. diagram of an absorber tube element.

Heat exchanges here take place between three elements which are: Heat transfer fluid, absorber and glass, as shown in **Figure 2**.

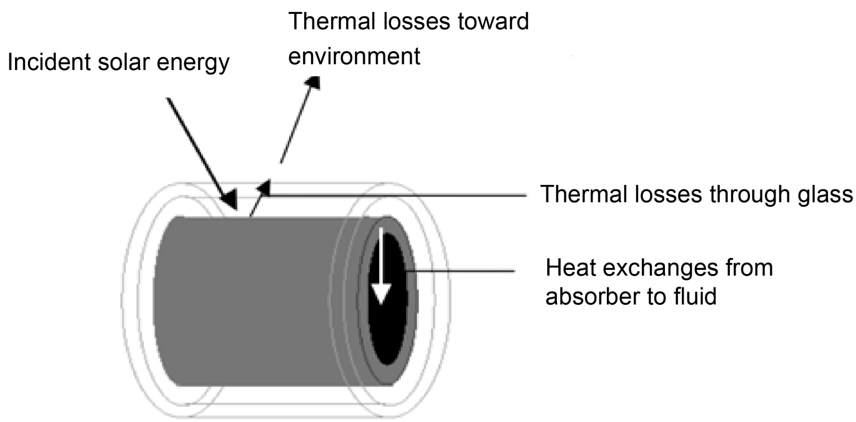

Figure 2. Schematic of heat transfer between different parts of parabolic collector.

3. Thermal Balance

3.1. Hypotheses

These assumptions are as follows:

- ✓ Collector follows sun perfectly;
- ✓ Flow of fluid in receiving tube is one-dimensional;
- ✓ Diameters of tubes and surface of collector are constant;
- ✓ Heat transfer by conduction in all elements of absorber is negligible;
- ✓ Heat transfer fluid is incompressible;
- ✓ Ambient temperature around parabolic trough is assumed to be uniform;
- ✓ Effect of shadow of absorber tube on glass is negligible;
- ✓ Solar flux at absorber is evenly distributed;
- ✓ Glass is considered opaque to infrared radiation;
- ✓ Temporal variations in thickness of absorber and glass are negligible.

Figure 3 below shows the diagram of an absorber on which a thermal balance is made.

3.2. Energy Balance in the Heat Transfer Fluid

Energy balance for heat transfer fluid circulating in absorber tube is expressed by the following relationship:

$$\frac{\partial}{\partial t}\left(\Delta Q_f\left(z,t\right)\right)=Q_f\left(z,t\right)-Q_f\left(z+\Delta z,t\right)+q_u\cdot\Delta z\left(z,t\right) \tag{1}$$

Heat quantity recovered by fluid $\Delta Q_f\left(z,t\right)$ in interval Δz is given by:

$$\Delta Q_f\left(z,t\right)=\rho_f\cdot C_f\cdot S_{ai}\cdot\Delta z\cdot T_f\left(z,t\right) \tag{2}$$

where:

ρ_f : fluid density;

C_f : specific heat of fluid;

$S_{ai}=\pi\cdot D_{ai}$: absorber internal exchange surface per unit length.

All thermo-physical properties of fluid depend on temperature T_f .

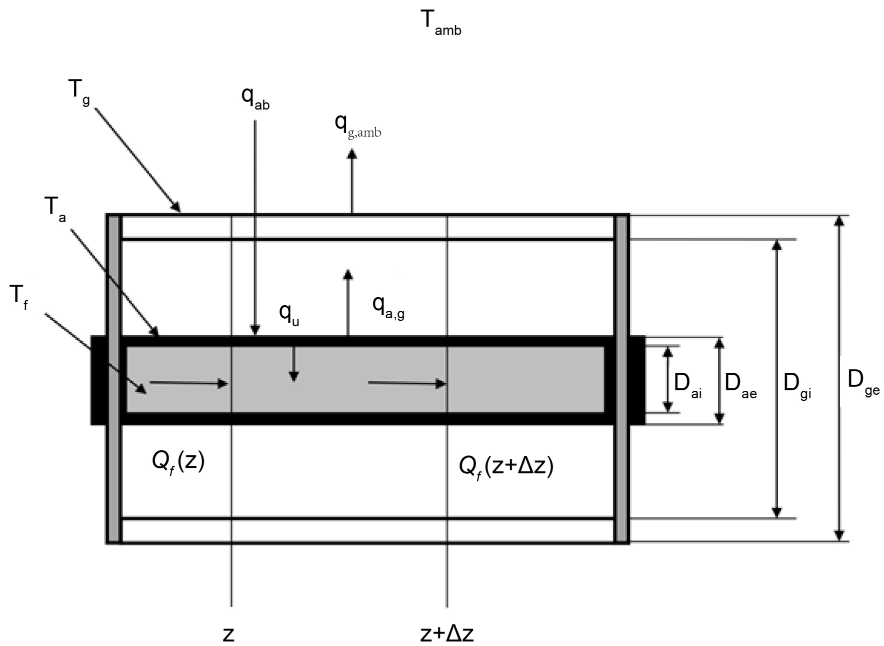

Figure 3. Absorber diagram. q_{ab}: heat quantity come from sun and receive by absorber; q_u: useful quantity heat transferred to coolant by absorber; $q_{a,v}$: quantity of heat exchanged by convection between absorber tube and glass; $q_{v,amb}$: heat quantity exchanged by convection between glass and ambient air; $Q_f(x)$: heat flow of heat transfer fluid at abscissa x; $Q_f(x+\Delta x)$: heat flow of heat transfer fluid at abscissa $x+\Delta x$; D_{ai}: internal diameter of absorber tube; D_{ae}: external diameter of absorber tube; D_{gi}: inside diameter of glass; D_{ge}: external diameter of glass; T_f: heat transfer fluid temperature; T_a: absorber temperature; T_g: glass temperature; $\dot{V}$: volume flow.

Heat quantity entering and leaving the element of length Δz is given by the following relations:

$$\begin{cases} Q_f(z,t) = \rho_f \cdot C_f \cdot \dot{V} \cdot T_f(z,t) \\ Q_f(z+\Delta z,t) = \rho_f \cdot C_f \cdot \dot{V} \cdot T_f(z+\Delta z,t) \end{cases} \tag{3}$$

Inserting Equations (2) and (3) into equation (1) gives the following relation (4):

$$\begin{aligned} &\rho_f \cdot C_f \cdot S_{ai} \cdot \Delta z \cdot \frac{\partial T_f}{\partial t}(z,t) \\ &= \rho_f \cdot C_f \cdot \dot{V} \cdot T_f(z,t) - \rho_f \cdot C_f \cdot \dot{V} \cdot T_f(z+\Delta z,t) + q_u(z,t) \cdot \Delta z \end{aligned} \tag{4}$$

The partial derivative with respect to abscissa z is:

$$\frac{\partial T_f}{\partial z}(z,t) = \frac{T_f(z+\Delta z,t) - T_f(z,t)}{\Delta z} \tag{5}$$

Divide Equation (4) by Δz and after substitution in Equation (5), we get:

$$\rho_f \cdot C_f \cdot S_{ai} \cdot \frac{\partial T_f}{\partial t}(z,t) = -\rho_f \cdot C_f \cdot \dot{V} \cdot \frac{\partial T_f}{\partial z}(z,t) + q_u(z,t) \tag{6}$$

Initial conditions and boundary conditions of Equation (6) are:

$$\begin{cases} T_f(0,t) = T_{f,inlet}(t) = T_{amb}(t) \\ T_f(z,0) = T_{f,initial}(z) = T_{amb}(0) \end{cases}$$

3.3. Energy Balance in the Absorber

The energy balance for absorber is given by the following relation:

$$\frac{\partial}{\partial t}\left(\Delta Q_a(z,t)\right) = \left(q_{ab}(t) - q_{a,g}(t) - q_u(t)\right)\cdot \Delta z \tag{7}$$

ΔQ_a: The amount of heat in absorber is expressed by:

$$\Delta Q_a(z,t) = \rho_a \cdot C_a \cdot S_{ae} \cdot \Delta z \cdot T_a(z,t) \tag{8}$$

where:

ρ_a: Density of the absorber;

C_a: Heat capacity of the absorber;

$S_{ae} = \pi \cdot D_{ae}$: absorber external exchange surface per unit length.

After substituting (8) in (7), we get the expression:

$$\rho_a \cdot C_a \cdot S_{ae} \cdot \frac{\partial T_a}{\partial t}(z,t) = q_{ab}(t) - q_{a,g}(t) - q_u(t) \tag{9}$$

Initial condition of Equation (9) is:

$$T_a(z,0) = T_{a,initial}(z) = T_{amb}(0)$$

3.4. Energy Balance in the Glass

The energy balance in the glass is given by:

$$\rho_g \cdot C_g \cdot S_g \cdot \frac{\partial T_g}{\partial t}(z,t) = q_{a,g}(t) - q_{g,amb}(t) \tag{10}$$

where:

ρ_g: glass density;

C_g: specific heat of glass;

$S_g = \pi \cdot D_g$: glass external exchange surface per unit length.

Initial condition of equation (10) is:

$$T_g(z,0) = T_{g,initial}(z) = T_{amb}(0)$$

4. Heat Exchanges

4.1. Heat Exchanges between Absorber and Fluid

We have:

$$q_u = h_f \cdot S_{ai}\left(T_a - T_f\right) \tag{11}$$

The convective exchange coefficient h_f essentially depends on fluid flow regime.

Its expression is:

$$h_f = \frac{Nu \cdot k_f}{D_{ai}} \tag{12}$$

where:

k_f : thermal conductivity of fluid;

Nu : Nusselt number, given by Gnielinsky correlation [18]:

$$Nu = \frac{(\chi/8)\left(Re_f - 1000\right)Pr_f}{1 + 12.7\sqrt{\chi/8}\left(Pr_f^{2/3} - 1\right)} \tag{13}$$

χ : is coefficient of friction calculated from Petukhov relation [18]:

$$\chi = \left(0.0790\ln\left(Re_f\right) - 1.64\right)^2 \tag{14}$$

Re_f : Reynolds number translated by the following relation [19]:

$$Re_f = \frac{4 \cdot \rho_f \cdot \dot{V}}{\pi \cdot \mu_f \cdot D_{ai}} \tag{15}$$

with: μ_f : dynamic fluid viscosity;

Pr_f : number of Prandtl given by the following expression:

$$Pr_f = \frac{\vartheta_f}{\alpha_f} \tag{16}$$

$\vartheta_f = \frac{\mu_f}{\rho_f}$: kinematic viscosity; $\alpha_f = \frac{k_f}{\rho_f \cdot C_f}$.

- ✓ For laminar flow ($Re_f < 2300$), Nusselt number is expressed by the following value [20]: $Nu = 4.36$;
- ✓ For turbulent flow ($Re_f > 2300$), Nusselt number is calculated by Gnielinsky correlation [18].

4.2. Heat Exchanges between Absorber and Glass

We have:

$$q_{a,g} = q_{a,g_{convection}} + q_{a,g_{radiation}} \tag{17}$$

Radiation exchange $q_{a,g_{radiation}}$ in annular space is given by Thorsten [19]:

$$q_{a,g_{radiation}} = \frac{\sigma \cdot S_{ae}\left(T_a^4 - T_g^4\right)}{\frac{1}{\varepsilon_a} + \frac{1-\varepsilon_g}{\varepsilon_g}\left(\frac{D_{ae}}{D_{gi}}\right)} \tag{18}$$

where:

$\sigma = 5.670 \times 10^{-8}\ \mathrm{W} \cdot \mathrm{m}^{-2} \cdot \mathrm{K}^{-4}$: Stefan Boltzmann's constant;

ε_a : absorber emissivity;

ε_g : glazing emissivity.

The internal heat exchange by convection in air space between absorber and glazing is given by [19], knowing that this air space is mobile:

$$q_{a,g_{convection}} = \frac{2\pi \cdot k_{eff,air}}{\ln\left(D_{gi}/D_{ae}\right)}\left(T_a - T_g\right) \tag{19}$$

where, $k_{eff,air}$ is equivalent thermal conductivity of air, given by:

$$\frac{k_{eff,air}}{k_{air}} = 0.386\left(\frac{Pr_{air}}{0.861+Pr_{air}}\right)^{1/4}\left(\frac{\left[\ln\left(D_{gi}/D_{ae}\right)\right]^4}{L^3\left(D_{ae}^{-3/5}+D_{gi}^{-3/5}\right)^3}Ra_L\right)^{1/4} \quad (20)$$

where:

L : average thickness of annular layer located between absorber and glass, equal to:

$$L = 0.5\left(D_{gi} - D_{ae}\right) \quad (21)$$

Ra_L : Rayleigh number for air, defined as follows [19]:

$$Ra_L = \frac{g \cdot \beta_{air}\left(T_a - T_g\right)L^3}{\alpha_{air} \cdot \vartheta_{air}} \quad (22)$$

where:

g : gravity intensity ($g = 9.81\,\mathrm{m \cdot s^{-2}}$);

β_{air} : thermal coefficient of volumetric expansion of air;

α_{air} : thermal diffusivity defined by:

$$\alpha_{air} = \frac{k_{air}}{\rho_{air} \cdot C_{p_{air}}} \quad (23)$$

$\rho_{air}, C_{p_{air}}, k_{air}$: are respectively density, specific heat at constant pressure and thermal conductivity of air;

ϑ_{air} : kinematic viscosity of air, expressed by: $\vartheta_{air} = \frac{\mu_{air}}{\rho_{air}}$;

where:

μ_{air} : dynamic air viscosity.

If in absence of convection (trapped air space is immobile) between absorber and glass, the flow per unit length is written [21]:

$$q_{a,g_{conduction}} = \frac{2\pi \cdot k_{air}}{\ln\left(D_{gi}/D_{ae}\right)}\left(T_a - T_g\right) \quad (24)$$

All thermodynamic properties of air in annulus ($k_{air}, Pr_{air}, \beta_{air}, \alpha_{air}, \vartheta_{air}, \rho_{air}, C_{p_{air}}, \mu_{air}$) depend on average temperature of annulus.

A semi-empirical equation is used for determination of average temperature of annular space for a cylindrical-shaped absorber [22]:

$$T_{average\ annular} = 320 + \left[\left(0.11 \times \varepsilon_a\right) + 0.57\right] \times \left(T_g - 320\right) \quad (25)$$

On other hand, average temperature in annular space, can be expressed by:

$$T_{average\ annular} = 0.5\left(T_g + T_a\right) \quad (26)$$

4.3. Heat Exchange between Glass and Surrounding Environment

It's assumed that heat transfer between transparent envelope (glass) and environment is also due to exchange by convection and radiation.

$$q_{g,amb} = q_{g,amb_{convection}} + q_{g,amb_{radiation}} \tag{27}$$

The amount of convective heat from glazing to environment is expressed by:

$$q_{g,amb_{convection}} = h_V \cdot S_{ge}\left(T_g - T_{amb}\right) \tag{28}$$

h_V : wind exchange coefficient, defined by the following expressions [22]:

$$\begin{cases} h_V = 5.7 + 3.8V_V & 0 < V_V < 4\ \text{m}\cdot\text{s}^{-1} \\ h_V = 7.3V_V^{0.8} & 4\ \text{m}\cdot\text{s}^{-1} < V_V < 40\ \text{m}\cdot\text{s}^{-1} \end{cases} \tag{29}$$

V_V : wind speed [m·s^{-1}].

The amount of heat radiating from glazing to environment can be expressed by the following relationship:

$$q_{v,amb_{radiation}} = \varepsilon_g \cdot \sigma \cdot S_{ge}\left(T_g^4 - T_{amb}^4\right) \tag{30}$$

5. Absorbed Energy

The thermal power emitted by sun and received by concentrator is [23]:

$$q_{ab} = S_e \cdot R_d\left(\beta\right) \tag{31}$$

S_e : effective area of a reflector of the parabolic trough;

$R_d\left(\beta\right)$: sunlight or direct radiation.

Since the surface of absorber S_a receives the same power as S_e, then the concentration has the effect of increasing power per unit area at the level of S_a; but due to optical losses around transparent envelope (glass) and absorber, the power per unit length of absorber is:

$$q_{ab} = \tau_v \cdot \alpha_{ab} \cdot \rho_m \cdot S_e \cdot R_d\left(\beta\right) \cdot k\left(\theta\right) \tag{32}$$

where:

ρ_m : Mirror reflectance factor;

α_{ab} : Absorption coefficient of absorber tube;

τ_g : Coverage transmission coefficient (glass);

$k\left(\theta\right)$: Angle of incidence modify.

For cylindro-parabolic collectors, the following equation [24], gives coefficient $k\left(\theta\right)$ as a function of angle of incidence:

$$k\left(\theta\right) = 1 - b_0\left(\frac{1}{\cos\left(\theta\right)}\right) \tag{33}$$

where:

b_0 : coefficient of modified angle less than zero for a cylindro-parabolic concentrator.

6. Thermal Power Losses in a Parabolic Trough Concentrator

The coefficient of thermal losses U_L is expressed by [25]:

$$U_L = \left(\frac{1}{C_1 \left[\left(T_a - T_{amb} \right) / \left(1 + \lambda \right) \right]^{0.25}} + \frac{D_{ai}}{D_{ae}} \times \frac{1}{h_V} \right)^{-1} + \frac{\sigma \left(T_a^2 + T_{amb}^2 \right) \left(T_a + T_{amb} \right)}{\left[\varepsilon_a - 0.04 \left(1 - \varepsilon_a \right) \left(T_a / 450 \right) \right]^{-1} - \left[\left(D_{ai} / D_{ae} \right) \left(1 / \varepsilon_g \right) + \lambda / \varepsilon_g \right]} \quad (34)$$

where:

λ : wind loss coefficient, obtained by equation (35):

$$\lambda = \frac{D_{ai}}{D_{ai}^{1.4}} \left(0.61 + 1.3 \varepsilon_a \right) h_g^{-0.9} \exp \left[0.00325 \left(T_a - 273 \right) \right] \quad (35)$$

$$C_1 = \frac{1.45 + 0.96 \left(\varepsilon_a - 0.5 \right)^2}{D_{ai} \left(1 / D_{ai}^{0.6} + D_{ae}^{0.6} \right)^{1.25}} \quad (36)$$

$$h_V = 4 V_V^{0.58} D_{ae}^{-0.42} \quad (37)$$

7. Numerical Solving

The finite difference method we use for our problem resolution, consists in approximating derivatives of equations obtained above, by means of Taylor expansions and is deduced directly from definition of derivative.

Discretization of one-dimensional equations (1D)

The space is discretized into $N+1$ nodes of coordinates z_j (j varying from 0 to N) regularly spaced. Note Δz the space step. Time is discretized in constant step intervals Δt.

Let us note T_j^n the temperature at the node $z_j = j\Delta z$ and at time $t = n\Delta t$.

We use an explicit before order 1 scheme to evaluate temporal and spatial derivative:

$$\left(\frac{\partial T}{\partial t} \right)_j^n = \frac{T_j^n - T_j^{n-1}}{\Delta t} \quad (38)$$

$$\left(\frac{\partial T}{\partial z} \right)_j^n = \frac{T_j^n - T_{j-1}^n}{\Delta z} \quad (39)$$

<u>For the fluid</u>

Equation (6) gives:

$$\rho_f \cdot C_f \cdot S_{ai} \cdot \frac{T_{f,j}^n - T_{f,j}^{n-1}}{\Delta t} = -\rho_f \cdot C_f \cdot \dot{V} \cdot \frac{T_{f,j}^n - T_{f,j-1}^n}{\Delta z} + q_u \left(z, t \right)$$

By replacing $q_u(z,t)$ by its expression and by expressing $T_{f,j}^n$ depending on other parameters, we get:

$$\left(1 + \frac{\Delta t \cdot \dot{V}}{\Delta z \cdot S_{ai}} + \frac{\Delta t}{\rho_f(j) C_f(j) S_{ai}} h_f \cdot S_{ai} \right) T_{f,j}^n + \frac{\Delta t}{\rho_f(j) C_f(j) S_{ai}} h_f \cdot S_{ai} T_{a,j}^n = \frac{C_f(j-1) \rho_f(j-1) \Delta t \cdot \dot{V}}{C_f(j) \rho_f(j) \Delta z \cdot S_{ai}} T_{f,j-1}^n + T_{f,j}^{n-1} \quad (40)$$

For the absorber

Equation (9) gives: $\rho_a \cdot C_a \cdot S_{ae} \cdot \frac{T_{a,j}^n - T_{a,j}^{n-1}}{\Delta t} = q_{ab}(t) - q_{a,g}(t) - q_u(t)$.

By replacing $q_{ab}(t)$, $q_{a,g}(t)$ and $q_u(t)$ by their expressions, we get:

$$\begin{aligned}
&\frac{\Delta t \cdot h_f \cdot S_{ai}}{\rho_a C_a S_{ae}} T_{f,j}^n \\
&+\left(1 - \frac{\Delta t}{\rho_a C_a S_{ae}}\left(\frac{2\pi \cdot k_{eff,air}}{\ln\left(D_{gi}/D_{ae}\right)} + h_f \cdot S_{ai} + \frac{\sigma \cdot S_{ae}\left(\left(T_{a,j}^2\right)^n + \left(T_{g,j}^2\right)^n\right)\left(T_{a,j}^n + T_{g,j}^n\right)}{\frac{1}{\varepsilon_a} + \frac{1-\varepsilon_g}{\varepsilon_g}\left(\frac{D_{ae}}{D_{gi}}\right)}\right)\right) T_{a,j}^n \\
&+\frac{\Delta t}{\rho_a C_a S_{ae}}\left(\frac{2\pi \cdot k_{eff,air}}{\ln\left(D_{gi}/D_{ae}\right)} + \frac{\sigma \cdot S_{ae}\left(\left(T_{a,j}^2\right)^n + \left(T_{g,j}^2\right)^n\right)\left(T_{a,j}^n + T_{g,j}^n\right)}{\frac{1}{\varepsilon_a} + \frac{1-\varepsilon_g}{\varepsilon_g}\left(\frac{D_{ae}}{D_{gi}}\right)}\right) T_{g,j}^n \\
&= T_{a,j}^{n-1} + \frac{\Delta t}{\rho_a C_a S_{ae}} \tau_g \cdot \alpha_{ab} \cdot \rho_m \cdot S_e \cdot R_d(\beta) \cdot k(\theta)
\end{aligned} \quad (41)$$

For the glass

Equation (10) gives: $\rho_g \cdot C_g \cdot S_g \cdot \frac{T_{g,j}^n - T_{g,j}^{n-1}}{\Delta t} = q_{a,g}(t) - q_{g,amb}(t)$.

By replacing $q_{a,g}(t)$ and $q_{g,amb}(t)$ by their expressions, we get:

$$\begin{aligned}
&-\frac{\Delta t}{\rho_g C_g S_g}\left(\frac{2\pi \cdot k_{eff,air}}{\ln\left(D_{gi}/D_{ae}\right)} + \frac{\sigma \cdot S_{ae}\left(\left(T_{a,j}^2\right)^n + \left(T_{g,j}^2\right)^n\right)\left(T_{a,j}^n + T_{g,j}^n\right)}{\frac{1}{\varepsilon_a} + \frac{1-\varepsilon_g}{\varepsilon_g}\left(\frac{D_{ae}}{D_{gi}}\right)}\right) T_{a,j}^n \\
&+\left(1 + \frac{\Delta t}{\rho_g C_g S_g}\left(\frac{2\pi \cdot k_{eff,air}}{\ln\left(D_{gi}/D_{ae}\right)} + \frac{\sigma \cdot S_{ae}\left(\left(T_{a,j}^2\right)^n + \left(T_{g,j}^2\right)^n\right)\left(T_{a,j}^n + T_{g,j}^n\right)}{\frac{1}{\varepsilon_a} + \frac{1-\varepsilon_g}{\varepsilon_g}\left(\frac{D_{ae}}{D_{gi}}\right)}\right.\right. \\
&\left.\left. + h_V \cdot S_{ge} + \varepsilon_g \cdot \sigma \cdot S_{ge}\left(\left(T_{g,j}^2\right)^n + \left(T_{amb,j}^2\right)^n\right)\left(T_{g,j}^n + T_{amb,j}^n\right)\right)\right) T_{g,j}^n \\
&= T_{g,j}^{n-1} + \frac{\Delta t}{\rho_g C_g S_g}\left(h_V \cdot S_{ge} + \varepsilon_g \cdot \sigma \cdot S_{ge}\left(\left(T_{g,j}^2\right)^n + \left(T_{amb,j}^2\right)^n\right)\left(T_{g,j}^n + T_{amb,j}^n\right)\right) T_{amb,j}^n
\end{aligned} \quad (42)$$

Equations (40), (41) and (42) form a system of equations with three unknowns to be solved.

It is also important to know that time step is one hour [26].

This system can be in the following matrix form:

$$\begin{bmatrix} b_1 & c_1 & 0 \\ a_2 & b_2 & c_2 \\ 0 & a_3 & b_3 \end{bmatrix} \begin{bmatrix} T_{f,j} \\ T_{a,j} \\ T_{v,j} \end{bmatrix}^n = \begin{bmatrix} d \\ e \\ g \end{bmatrix}$$

where:

$$b_1 = 1 + \frac{\Delta t \cdot \dot{V}}{\Delta z \cdot S_{ai}} + \frac{\Delta t}{\rho_f(j) C_f(j) S_{ai}} h_f \cdot S_{ai}$$

$$c_1 = \frac{\Delta t}{\rho_f(j) C_f(j) S_{ai}} h_f \cdot S_{ai}$$

$$d = \frac{C_f(j-1)\rho_f(j-1)\Delta t \cdot \dot{V}}{C_f(j)\rho_f(j)\Delta z \cdot S_{ai}} T_{f,j-1}^n + T_{f,j}^{n-1}$$

$$a_2 = \frac{\Delta t \cdot h_f \cdot S_{ai}}{\rho_a C_a S_{ae}}$$

$$b_2 = 1 - \frac{\Delta t}{\rho_a C_a S_{ae}} \left(\frac{2\pi \cdot k_{eff,air}}{\ln(D_{gi}/D_{ae})} + h_f \cdot S_{ai} + \frac{\sigma \cdot S_{ae}\left(\left(T_{a,j}^2\right)^n + \left(T_{g,j}^2\right)^n\right)\left(T_{a,j}^n + T_{g,j}^n\right)}{\frac{1}{\varepsilon_a} + \frac{1-\varepsilon_g}{\varepsilon_g}\left(\frac{D_{ae}}{D_{gi}}\right)} \right)$$

$$c_2 = \frac{\Delta t}{\rho_a C_a S_{ae}} \left(\frac{2\pi \cdot k_{eff,air}}{\ln(D_{gi}/D_{ae})} + \frac{\sigma \cdot S_{ae}\left(\left(T_{a,j}^2\right)^n + \left(T_{g,j}^2\right)^n\right)\left(T_{a,j}^n + T_{g,j}^n\right)}{\frac{1}{\varepsilon_a} + \frac{1-\varepsilon_g}{\varepsilon_g}\left(\frac{D_{ae}}{D_{gi}}\right)} \right)$$

$$e = T_{a,j}^{n-1} + \frac{\Delta t}{\rho_a C_a S_{ae}} \tau_g \cdot \alpha_{ab} \cdot \rho_m \cdot S_e \cdot R_d(\beta) \cdot k(\theta)$$

$$a_3 = -\frac{\Delta t}{\rho_g C_g S_g} \left(\frac{2\pi \cdot k_{eff,air}}{\ln(D_{gi}/D_{ae})} + \frac{\sigma \cdot S_{ae}\left(\left(T_{a,j}^2\right)^n + \left(T_{g,j}^2\right)^n\right)\left(T_{a,j}^n + T_{g,j}^n\right)}{\frac{1}{\varepsilon_a} + \frac{1-\varepsilon_g}{\varepsilon_g}\left(\frac{D_{ae}}{D_{gi}}\right)} \right)$$

$$b_3 = 1 + \frac{\Delta t}{\rho_g C_g S_g} \left(\frac{2\pi \cdot k_{eff,air}}{\ln(D_{gi}/D_{ae})} + \frac{\sigma \cdot S_{ae}\left(\left(T_{a,j}^2\right)^n + \left(T_{g,j}^2\right)^n\right)\left(T_{a,j}^n + T_{g,j}^n\right)}{\frac{1}{\varepsilon_a} + \frac{1-\varepsilon_g}{\varepsilon_g}\left(\frac{D_{ae}}{D_{gi}}\right)} \right.$$

$$\left. + h_V \cdot S_{ge} + \varepsilon_g \cdot \sigma \cdot S_{ge}\left(\left(T_{g,j}^2\right)^n + \left(T_{amb,j}^2\right)^n\right)\left(T_{g,j}^n + T_{amb,j}^n\right) \right)$$

$$g = T_{g,j}^{n-1} + \frac{\Delta t}{\rho_g C_g S_g}\left(h_V \cdot S_{ge} + \varepsilon_g \cdot \sigma \cdot S_{ge}\left(\left(T_{g,j}^2\right)^n + \left(T_{amb,j}^2\right)^n\right)\left(T_{g,j}^n + T_{amb,j}^n\right)\right) T_{amb,j}^n$$

Which give: $[A][T] = [B]$.

Or $[A]=\begin{bmatrix} b_1 & c_1 & 0 \\ a_2 & b_2 & c_2 \\ 0 & a_3 & b_3 \end{bmatrix}$; $[T]=\begin{bmatrix} T_{f,j} \\ T_{a,j} \\ T_{v,j} \end{bmatrix}$; $[B]=\begin{bmatrix} d \\ e \\ g \end{bmatrix}$.

The matrix A of system being tridiagonal, we will use Gaussian pivot method for resolution of our problem.

Computation is carried out in two stages: triangularization and determination of unknowns.

Which give:

$$T_{a,j}^{n}=\frac{b_1\left(eb_3-c_2g\right)-b_3a_2d}{b_1\left(b_2b_3-c_1a_2\right)-b_2c_2a_3}$$

$$T_{f,j}^{n}=\frac{db_1\left(b_2b_3-c_1a_2\right)-db_2c_2a_3-c_1b_1\left(eb_3-c_2g\right)+c_1b_3a_2d}{b_1^2\left(b_2b_3-c_1a_2\right)-b_1b_2c_2a_3}$$

$$T_{g,j}^{n}=\frac{gb_1\left(b_2b_3-c_1a_2\right)-gb_2c_2a_3-a_3b_1\left(eb_3-c_2g\right)+a_3b_3a_2d}{b_3b_1\left(b_2b_3-c_1a_2\right)-b_3b_2c_2a_3}$$

8. Parameters Used in Numerical Simulation

Table 1 and Table 2 group together the geometric and optical characteristics of our cylindro-parabolic concentrator.

Table 1. Geometric parameters.

Geometric characteristics	Value
Internal diameter of absorber	0.1 m
External diameter of absorber	0.12 m
Internal diameter of glass	0.2 m
External diameter of glass	0.24 m
Effective mirror width	2 m/1 m/0.5 m
Number of collector, N_{col}	1
Length element, Δz	0.1 m
Tube length of each manifold, L_{tube}	2 m
Focal distance	0.235 m

Table 2. Optical properties of materials.

Optical properties of materials used	Value
Absorption coefficient of absorber tube, α	0.8
Glass transmittivity, τ_g	0.8
Mirror surface reflectance, ρ_m	0.85
Emissivity of the absorber tube (visible), ε_a	0.12
Glass tube emissivity, ε_g	0.9

A computer program written in Matlab language has been developed to simulate outlet temperature of heat transfer fluid, absorber and glass of cylindro-parabolic solar concentrator.

9. Result and Discussion

In this part, we present results of numerical simulation, as well as the effect of some geometric and climatic parameters [12] on evolution of outlet temperature T_f.

9.1. Evolution of Outlet Temperature

Figure 4 shows the variation in temperatures of fluid, absorber and glass at outlet of absorber tube as a function of time.

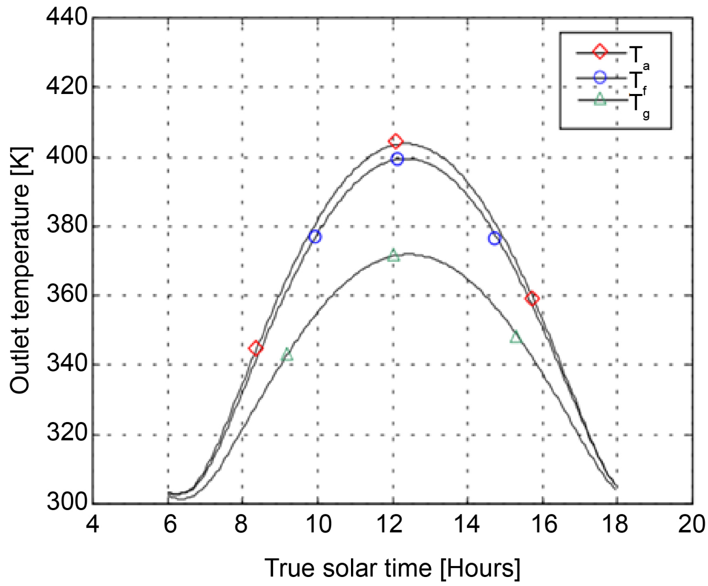

Figure 4. Outlet temperature evolution of fluid (T_f), absorber (T_a) and glass (T_g) for March 21.

- For a typical day of year, for a constant volume flow, outlet temperature of heat transfer fluid reaches its maximum value around 400 K recorded at true solar noon for day of March 21. It mainly depends on $q_{ab}(t)$, which is a function of optical and geometric parameters of concentrator and of direct radiation received by sensor.
- Note that temperature of absorber (T_a) is almost close to temperature (T_f) of fluid, which can reach 405 K at true solar noon for day of March 21. This can be justified by its high absorption power for visible solar radiation and low emissivity for long-wavelength infrared radiation, which is provided by its coating. It is possible to conserve most of incident solar energy and lose very little heat by long-wavelength radiation when absorbent surface becomes hot.
- The glazing temperature (T_v) is lower than (T_a) and (T_f) which can reach 375K

at true solar noon for day of March 21, because internal face of glass absorbs infrared radiation, which undergoes an increase of temperature (T_v) (greenhouse effect). Therefore that of external face is lower, which is close to the ambient environment subjected mainly to the speed of wind, which creates a phenomenon of convection on glass outside.

9.2. Effects of Geometric Parameters on Fluid Temperature

9.2.1. Influence of Absorber Length

Figure 5 represents fluid temperature variation at the outlet as a function of length of absorber tube for three values of direct radiation (1000 W/m², 700 W/m² and 500 W/m²). Note that increase in fluid temperature (T_f) is proportional to length and intensity of solar flow.

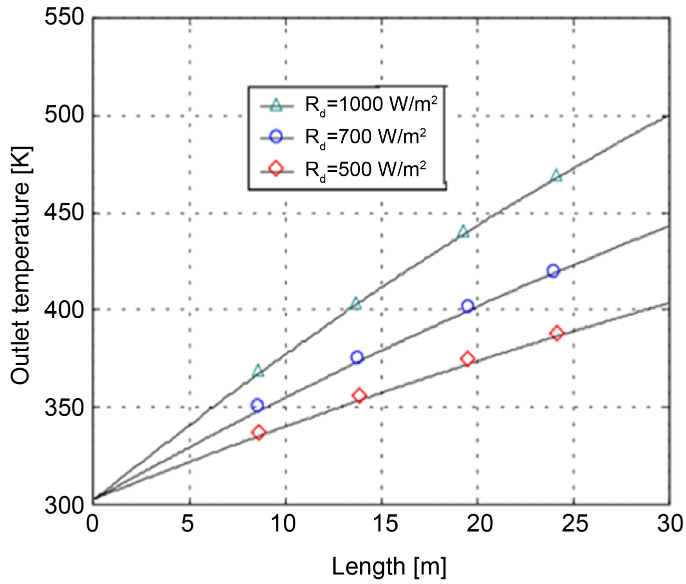

Figure 5. outlet temperature evolution as a function of length of absorber tube.

9.2.2. Effect of Reflector Width (Concentrator Opening)

To see the effect of width of mirror on fluid temperature (T_f), we have chosen three values, 2 m, 1 m and 0.5 m, where we notice in Figure 6, the maximum value of (T_f) corresponds to the width of 2 m (570 K) for day of March 21.

9.3. Thermal Losses

Absorber is the site of thermal losses [11]. Figure 7 shows change in coefficient of heat losses as a function of average temperature of absorber for three values of emissivity ε_p: 0. 9, 0.5 and 0.2. Note that losses increase with increase of absorber average temperature. The emissivity of 0.2 could further reduce radiation losses by adopting selective surfaces. Eliminating air between transparent glass casing and absorber (creating a vacuum) could significantly reduce convection losses.

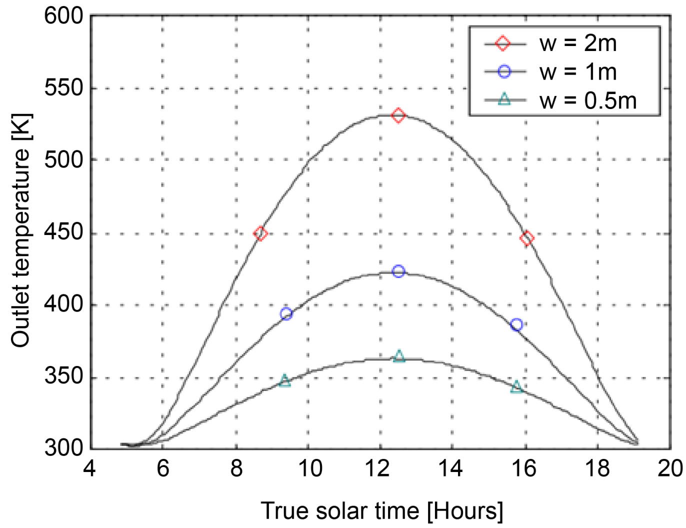

Figure 6. Evolution of temperature T_f of fluid as a function of width of mirror.

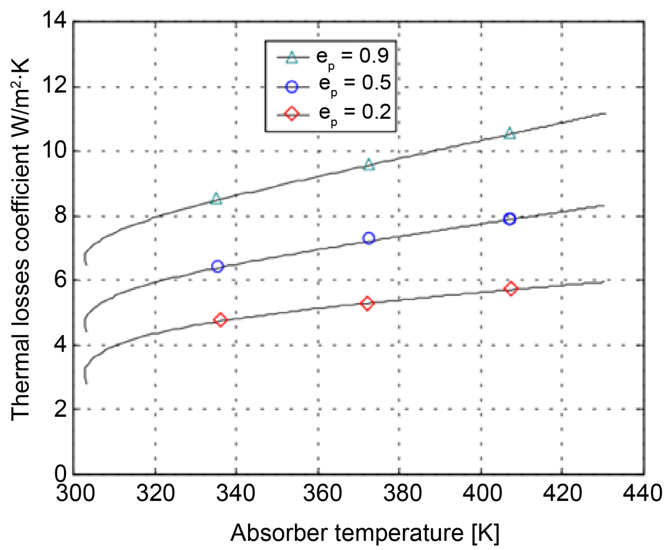

Figure 7. Evolution of coefficient of thermal losses as a function of absorber temperature for different emissivities.

10. Conclusions

The aim of our work was to model a parabolic trough concentrator, to numerically solve the resulting equation and to simulate the heating process of the heat transfer fluid.

Thus, a heat balance was established for the heat transfer fluid, the absorber and the glass. This allowed us to establish a system of equations whose resolution was done by the finite difference method. Then, a computer program was developed to simulate the temperatures of the heat transfer fluid, the absorber tube and the glass as a function of time and space.

The simulation of the fluid heating process was done in one-hour time steps, from 6 am to 6 pm. The results obtained show that the temperature difference between the inlet and outlet of the sensor is very large, thus making it possible to increase the power and efficiency of the parabolic trough concentrator.

Conflicts of Interest

The authors declare no conflicts of interest regarding the publication of this paper.

References

[1] Khireddine, B. and Cherif, B. (2016) Etude numérique tridimensionnelle des caractéristiques thermiques du tube absorbeur d'un capteur solaire cylindro-parabolique. 3*rd International Conference on Energy*, *Materials*, *Applied Energetics and Pollution ICEMAEP* 2016, Algeria, 30-31 October 2016, 555-560.

[2] Mahinder Singh, B.S. and Sulaiman, F. (2003) Designing a Solar Thermal Cylindrical Parabolic Trough Concentrator by Simulation. *World Climate & Energy Event*, **2003**, 143-149.

[3] Arnaoutakis, G.E. and Katsaprakakis, D.A. (2021) Concentrating Solar Power Advances in Geometric Optics, Materials and System Integration. *Energies*, **14**, Article 6229. https://doi.org/10.3390/en14196229

[4] Katsaprakakis, D. (2019) Introducing a Solar-Combi System for Hot Water Production and Swimming Pools Heating in the Pancretan Stadium, Crete, Greece. *Energy Procedia*, **159**, 174-179. https://doi.org/10.1016/j.egypro.2018.12.047

[5] Odeh, S.D., Behnia, M. and Morrison, G.L. (2003) Performance Evaluation of Solar Thermal Electric Generation Systems. *Energy Conversion and Management*, **44**, 2425-2443. https://doi.org/10.1016/s0196-8904(03)00011-6

[6] Adel, L. (2021) Amélioration des échanges thermiques dans l'absorbeur d'un concentrateur solaire cylindro-parabolique. Thèse de Doctorat, Université Hadj Lakhdar.

[7] Mwesigye, A. and Meyer, J.P. (2017) Optimal Thermal and Thermodynamic Performance of a Solar Parabolic Trough Receiver with Different Nanofluids and at Different Concentration Ratios. *Applied Energy*, **193**, 393-413. https://doi.org/10.1016/j.apenergy.2017.02.064

[8] Bitam, E.W., Demagh, Y., Hachicha, A.A., Benmoussa, H. and Kabar, Y. (2018) Numerical Investigation of a Novel Sinusoidal Tube Receiver for Parabolic Trough Technology. *Applied Energy*, **218**, 494-510. https://doi.org/10.1016/j.apenergy.2018.02.177

[9] Gong, X., Wang, F., Wang, H., Tan, J., Lai, Q. and Han, H. (2017) Heat Transfer Enhancement Analysis of Tube Receiver for Parabolic Trough Solar Collector with Pin Fin Arrays Inserting. *Solar Energy*, **144**, 185-202. https://doi.org/10.1016/j.solener.2017.01.020

[10] Bellos, E. and Tzivanidis, C. (2018) Enhancing the Performance of Evacuated and Non-Evacuated Parabolic Trough Collectors Using Twisted Tape Inserts, Perforated Plate Inserts and Internally Finned Absorber. *Energies*, **11**, Article 1129. https://doi.org/10.3390/en11051129

[11] Bellos, E., Tzivanidis, C. and Tsimpoukis, D. (2018) Optimum Number of Internal Fins in Parabolic Trough Collectors. *Applied Thermal Engineering*, **137**, 669-677. https://doi.org/10.1016/j.applthermaleng.2018.04.037

[12] Benzenine, H., Saim, R., Abboudi, S., Imine, O., Oztop, H.F. and Abu-Hamdeh, N.

(2018) Numerical Study of a Three-Dimensional Forced Laminar Flow in a Channel Equipped with a Perforated Baffle. *Numerical Heat Transfer*, *Part A*: *Applications*, **73**, 881-894. https://doi.org/10.1080/10407782.2018.1486645

[13] García-Valladares, O. and Velázquez, N. (2009) Numerical Simulation of Parabolic Trough Solar Collector: Improvement Using Counter Flow Concentric Circular Heat Exchangers. *International Journal of Heat and Mass Transfer*, **52**, 597-609. https://doi.org/10.1016/j.ijheatmasstransfer.2008.08.004

[14] Fernández-García, A., Zarza, E., Valenzuela, L. and Pérez, M. (2010) Parabolic-trough Solar Collectors and Their Applications. *Renewable and Sustainable Energy Reviews*, **14**, 1695-1721. https://doi.org/10.1016/j.rser.2010.03.012

[15] Campo, A. (2005) Quick Identification of Gases for Enhancing Heat Transfer in Turbulent Pipe Flows Using Standard Correlation Equations for the Convective Coefficient and the Friction Factor. *Applied Thermal Engineering*, **25**, 2029-2038. https://doi.org/10.1016/j.applthermaleng.2004.02.015

[16] Grald, E.W. and Kuehn, T.H. (1989) Performance Analysis of a Parabolic Trough Solar Collector with a Porous Absorber Receiver. *Solar Energy*, **42**, 281-292. https://doi.org/10.1016/0038-092x(89)90030-3

[17] Iqbal, M. (1983) An Introduction to Solar Energy. Academic Press.

[18] Lienhard, J.H. (2003) A Heat Transfer Textbook. 3rd Edition, Dover Publications.

[19] Stuetzele, T.A. (2002) Automatic Control of the 30 Mwe SEGS VI Parabolic Trough Plant. Master's Thesis, University of Wisconsin.

[20] Ammari, H.D. and Nimir, Y.L. (2003) Experimental and Theoretical Evaluation of the Performance of a Tar Solar Water Heater. *Energy Conversion and Management*, **44**, 3037-3055. https://doi.org/10.1016/s0196-8904(03)00076-1

[21] Petit, J.-P. (1989-1990) Convection Naturelle, Ecole Centrale Paris.

[22] Merzaka, A. (2002) Simulation et prédiction des pertes thermiques d'un Absorbeur pour un concentrateur cylindro-parabolique. Thèse de magister, Batna.

[23] Alphilippe, B.M. and Stouffs, P. (2003) Conversion thermodynamique de l'énergie solaire dans des installations de faible ou de moyenne puissance: Réflexion sur choix du meilleur degré de concentration. https://www.academia.edu/66681454/Conversion_Thermodynamique_de_lEnergie_Solaire_dans_des_Installations_de_Faible_ou_de_Moyenne_Puissance_R%C3%A9flexions_sur_le_Choix_du_Meilleur_Degr%C3%A9_de_Concentration

[24] Das, T. and Pramanik, K. (2004) Modelling and Performance Evaluation of Solar Water Heating Systems. *Word Renewable Energy Congress VIII*, *WREC* 2004, Denver, 29 August-3 September 2004, 504.

[25] Mullick, S.C. and Nanda, S.K. (1989) An Improved Technique for Computing the Heat Loss Factor of a Tubular Absorber. *Solar Energy*, **42**, 1-7. https://doi.org/10.1016/0038-092x(89)90124-2

[26] Klein, S.A., Duffie, J.A. and Beckman, W.A. (1974) Transient Considerations of Flat-Plate Solar Collectors. *Journal of Engineering for Power*, **96**, 109-113. https://doi.org/10.1115/1.3445757